Lipid nanocapsules decorated and loaded with cannabidiol as targeted prolonged release carriers for glioma therapy: *in vitro* screening of critical parameters

Juan Aparicio-Blanco, Víctor Sebastián, Jean P. Benoit, Ana I. Torres-Suárez

PII: S0939-6411(18)31136-6
DOI: https://doi.org/10.1016/j.ejpb.2018.11.020
Reference: EJPB 12935

To appear in: *European Journal of Pharmaceutics and Biopharmaceutics*

Received Date: 14 September 2018
Revised Date: 17 November 2018
Accepted Date: 21 November 2018

Please cite this article as: J. Aparicio-Blanco, V. Sebastián, J.P. Benoit, A.I. Torres-Suárez, Lipid nanocapsules decorated and loaded with cannabidiol as targeted prolonged release carriers for glioma therapy: *in vitro* screening of critical parameters, *European Journal of Pharmaceutics and Biopharmaceutics* (2018), doi: https://doi.org/10.1016/j.ejpb.2018.11.020

Lipid nanocapsules decorated and loaded with cannabidiol as targeted prolonged release carriers for glioma therapy: *in vitro* screening of critical parameters

Juan Aparicio-Blanco [a], Víctor Sebastián [b, c], Jean P. Benoit [d], Ana I. Torres-Suárez [a, e,*]

[a] Department of Pharmaceutics and Food Technology, Complutense University, Madrid, Spain

[b] Department of Chemical Engineering, Aragon Institute of Nanoscience (INA), University of Zaragoza, Zaragoza, Spain

[c] Networking Research Center on Bioengineering, Biomaterials and Nanomedicine (CIBER-BBN), Madrid, Spain

[d] MINT, UNIV Angers, INSERM 1066, CNRS 6021, Université Bretagne Loire, Angers, France

[e] University Institute of Industrial Pharmacy, Complutense University, Madrid, Spain

[*]Corresponding author: Prof. Ana I. Torres-Suárez

Telephone: +34 91 394 1735; e-mail: galaaaa@ucm.es

Abstract

The therapeutic potential of cannabinoids has been truly constrained heretofore due to their strong psychoactive effects and their high lipophilicity. In this context, precisely due to the lack of psychoactive properties, cannabidiol (CBD), the second major component of *Cannabis sativa*, arises as the phytocannabinoid with the most auspicious therapeutic potential. Hence, the incorporation of CBD in lipid nanocapsules (LNCs) will contribute to overcome the dosing problems associated with cannabinoids.

Herein, we have prepared LNCs decorated and loaded with CBD for glioma therapy and screened *in vitro* their critical parameters. On the one hand, we have encapsulated CBD into the oily core of LNCs to test their *in vitro* efficacy as extended-release carriers against the human glioblastoma cell line U373MG. The *in vitro* antitumor effect was highly dependent on the size of LNCs due to its pivotal role in the extent of CBD release. Effectively, a comparison between two differently-sized LNCs (namely, 20-nm and 50-nm sized carriers) showed that the smaller LNCs reduced by 3.0-fold the IC_{50} value of their 50-nm sized counterparts. On the other hand, to explore the potential of this phytocannabinoid to target any of the cannabinoid receptors overexpressed in glioma cells, we decorated the LNCs with CBD. This functionalization strategy enhanced the *in vitro* glioma targeting by 3.4-fold in comparison with their equally-sized undecorated counterparts. Lastly, the combination of CBD-loading with CBD-functionalization further reduced the IC_{50} values. Hence, the potential of these two strategies of CBD incorporation into LNCs deserves subsequent *in vivo* evaluation.

Keywords

Cannabinoids, lipid-based carriers, glioma targeting, extended-release, glioblastoma

1. Introduction

Cannabis sativa is an herbaceous plant that contains over one hundred distinct pharmacologically-active terpenophenols that are produced in its glandular trichomes [1]. These compounds are known as phytocannabinoids since they chiefly exert their pharmacological effect on cannabinoid receptors. Other two types of cannabinoids are currently acknowledged: endocannabinoids, produced naturally by animals and humans, and synthetic cannabidomimetics.

Various cannabinoids produce strong psychoactive effects, which have truly constrained their therapeutic potential. As a proof of it, the marketing authorization of rimonabant, a synthetic cannabidomimetic that had been approved as anorectic for obese patients, was withdrawn in 2009 due to its severe psychiatric side effects. Fortunately, cannabidiol (CBD), the second major component of *Cannabis sativa*, with the tetrahydrofuran ring cleaved, is devoid of psychoactive properties. Precisely due to this lack of psychoactive effects, CBD is doubtless the most auspicious phytocannabinoid for the treatment of various pathologies, namely inflammatory and neurodegenerative diseases, mental disorders, neuropathic pain, epilepsy and cancer [2]. In the latter case, apart from palliating cancer-related symptoms (such as nausea, pain or anorexia), CBD has been reported to promote apoptotic cancer cell death through the production of reactive oxygen species, to impair tumor angiogenesis and to reduce cell migration that ultimately accounts for metastasis [3-5]. Particularly, the expression of different receptors to which the phytocannabinoids bind is increased in glioma (cannabinoid receptors 1 and 2 (CB1 and CB2) [6] and transient potential vanilloid receptor type 2 (TRPV2) [7]). Accordingly, activation of these receptors by CBD induced apoptosis of glioma cells, while no effects were observed in normal human astrocytes [7, 8].

Glioblastomas are the most prevalent and aggressive type of glioma (classified as the highest malignancy grade of gliomas by the World Health Organisation due to their high proliferative potential and invasiveness) [9]. Since the current standard of care of glioblastoma remains questionable, with a poor median survival of 14.6 months and a 2-year survival rate of 26.5% [10], CBD can serve to widen the therapeutic armamentarium for the treatment of malignant brain tumors thanks to its synergistic effects with the currently available chemo and radiotherapy [11]. As a proof of it, CBD has already reached the clinical trials stage in combination with chemo and/or radiotherapy for patients with glioblastoma (NCT01812616, NCT01812603, NCT03246113, NCT03529448, NCT03607643 and NCT03687034).

Nonetheless, the high lipophilicity of cannabinoids, including CBD, has also hampered their therapeutic potential. In this context, these substances can take great advantage of nanomedicine-based formulation strategies. Consistently, several studies on nanocarriers encapsulating the different kinds of cannabinoids (phytocannabinoids [12-14], cannabidomimetics [15-18], and endocannabinoids [19]) have started being published with distinct therapeutic purposes. Notwithstanding that for cannabinoids to achieve high translational impact they should be devoid of psychoactive effects, the

focus so far has been mainly put on the encapsulation of 9-delta-tetrahydrocannabinol (Δ^9-THC) and its analogues.

Herein, we develop monodisperse lipid nanocapsules (LNCs) as biocompatible and biodegradable carriers for CBD, the major non-psychotropic phytocannabinoid. LNCs are prepared by the energetically efficient phase inversion temperature (PIT) method. We encapsulate CBD into the oily core of LNCs at high drug loading, under the assumption that it would help overcome classical formulation issues linked to cannabinoids and attain a platform for its prolonged release after administration. Their *in vitro* efficacy against the human glioblastoma cell line U373MG is evaluated by means of cell viability experiments. The role played by the size of LNCs in CBD release and cytotoxicity is likewise thoroughly explored. Moreover, we evaluate the possibilities of this cannabinoid to target any of the cannabinoid receptors overexpressed in glioma cells as aforementioned. To this end, we develop a functionalization strategy of LNCs with CBD wherewith subsequently conduct uptake experiments on the same human glioblastoma cell line to evidence the potential targeting efficiency of this strategy.

2. Materials and methods

2.1. Materials

Labrafac® lipophile WL 1349 (caprylic-capric acid triglycerides) was kindly supplied by Gattefossé. Kolliphor® HS15 ($C_{18}E_{15}$ polyethylene glycol (15) 12-hydroxystearate) was a gift from BASF. Lipoid® S75 (soybean lecithin with 70% of phosphatidylcholine) was supplied by Lipoid-Gmbh. NaCl was purchased from Panreac. De-ionized water was obtained from a MilliQ® Purification System. The fluorescent dye 3,3'-dioctadecyloxacarbocyanine perchlorate (DiO) was purchased from Invitrogen Molecular Probes. Cannabidiol (CBD) was provided by THC-Pharma. Methanol, acetonitrile and tetrahydrofuran HPLC grade were purchased from Fisher Scientific. Amicon® Ultra 15 mL Centrifugal Filters (MWCO: 10 kDa) were supplied by Merck Millipore. Dulbecco's Modified Eagle Medium (DMEM) and penicillin-streptomycin (10,000 U/mL) were provided by Gibco. Fetal bovine serum (FBS) was supplied by Biowest. Hank's Balanced Salt Solution (HBSS), 3-(4,5-dimethyl-2-thiazolyl)-2,5-diphenyl-2H-tetrazolium bromide (MTT), dimethyl-sulfoxide (DMSO) and sterile Nunc Lab-Tek® chamber slides (8 wells, Permanox® slide, 0.8 cm^2/well) were purchased from Sigma-Aldrich. Vectashield® mounting medium with DAPI (H-1200) was provided by Vector Laboratories.

2.2. Cell line

The human glioblastoma U373MG cells were cultured in DMEM medium supplemented with 10% FBS, 100 U/mL penicillin and 100 μg/mL streptomycin at 37ºC in a humidified atmosphere containing 5% CO_2. For all experiments, cells between passage 15 and 25 were used.

2.3. Preparation of LNCs

2.3.1. Blank LNCs

LNCs were prepared by the PIT method. Succinctly, Labrafac® WL 1349, Kolliphor® HS15, Lipoid® S75, NaCl and water were mixed under magnetic stirring and progressively heated over the phase inversion temperature of the system. Subsequently, the mixture was gradually cooled down until the phase inversion temperature was reached. Then, a sudden quench with cold water (5 mL) was performed to obtain the final suspension of LNCs. By varying the relative proportions of the excipients, formulations of blank LNCs in different sizes were prepared.

2.3.2. CBD-loaded LNCs

CBD was encapsulated in LNCs for *in vitro* efficacy experiments. To prepare the CBD-loaded LNCs, the cannabinoid was firstly dissolved in the oily phase that constitutes the core of the LNCs at a concentration of 15 % CBD/ Labrafac® WL1349 (w/w). Then, the remaining excipients were added and progressively heated and cooled down around the phase inversion temperature as indicated in 2.3.1.

2.3.3. Fluorescently-labeled LNCs

The fluorescent dye DiO was encapsulated in LNCs for particle tracking purposes in *in vitro* experiments. To prepare the dye-loaded LNCs, the fluorescent dye was firstly dissolved in the oily phase that constitutes the core of the LNCs at a weight ratio of 15 mg of dye/ g of Labrafac® WL1349. Then, the remaining excipients were added and progressively heated and cooled down around the phase inversion temperature as indicated in 2.3.1.

2.3.4. Functionalization of LNCs with CBD

Pre-formed blank LNCs were incubated with a CBD solution to ultimately obtain functionalized LNCs at two different concentrations of CBD (10 mg/mL in a 1:4 (v/v) ratio for a final CBD concentration of 2.5 mg/mL, and 15 mg/mL in a 1:3 (v/v) ratio for a final CBD concentration of 5 mg/mL, respectively). The mixture was gently stirred overnight until complete solvent evaporation. The contribution of the solvent itself to the size distribution of LNCs was ruled out by incubating LNCs with pure solvent. Similarly, fluorescently-labeled and CBD-loaded LNCs were also functionalized with CBD at the higher concentration (5 mg/mL).

The detailed excipient weight for each group of LNCs is shown in Table 1: blank LNCs (F1-F3), CBD-loaded LNCs (F4-F6), CBD-functionalized LNCs (2.5 mg/mL –F7-F9- and 5 mg/mL –F10-F12), fluorescently-labeled LNCs (F13-F16) and CBD-functionalized-CBD-loaded LNCs (F17 and F18).

2.4. Characterization of LNCs

2.4.1. Size distribution and zeta potential

The average volume diameter and polydispersity index (PdI) of each formulation were measured by dynamic light scattering (DLS) using a Microtrac® Zetatrac™ Analyzer (Microtrac Inc., USA). Measurements were done in triplicate. The

zeta potential of the different formulations of LNCs was measured by means of a Zetasizer Nano ZS (Malvern Instruments).

2.4.2. Morphological examination of LNCs

The morphological examination of LNCs was performed by transmission electron microscopy (TEM). TEM images were taken on a T20-FEI Tecnai thermionic microscope at the Advanced Microscopy Laboratory, LMA, (Zaragoza, Spain). To prepare the samples for TEM, 20 µl of lipid nanocapsule suspension was dropped on a carbon copper grid (200 mesh), negatively stained with phosphotungstic acid and dried at room temperature. The microscope was operated at an acceleration voltage of 200 kV.

2.4.3. Incorporation efficiency and drug content

The incorporation efficiency (IE) and drug content (DC) of CBD in the different formulations of LNCs were determined by high performance liquid chromatography (HPLC). The HPLC method was adapted from [20]. An Agilent 1200 Infinity HPLC system was utilized. A mixture of methanol: acetonitrile: water (52:30:18 v/v) at a flow rate of 1.8 mL/min was used as mobile phase. The analytical column was a reversed-phase Mediterranea Sea® C18 (5µm 15 x 0,46 cm) (Teknokroma®). The retention time of CBD was 5 minutes.

The incorporation efficiency was calculated using equation 1, whereas the drug content was calculated using equation 2:

$$IE(\%) = \frac{Amount\ of\ CBD\ associated\ with\ LNCs}{Amount\ of\ CBD\ initally\ added} x100 \text{ (Equation 1)}$$

$$DC(\%) = \frac{Amount\ of\ CBD\ associated\ with\ LNCs}{Nanocapsule\ excipients' weight} x100 \text{ (Equation 2)}$$

where the amount of CBD associated with LNCs in each case was determined as the difference between the total amount of CBD in suspension derived from the lysis of LNCs with tetrahydrofuran (1:5 (v/v)) and the unassociated CBD filtered with 10 kDa Amicon® Centrifugal Filters (6000 rpm, 60 min).

2.5. *In vitro* cytotoxicity

Free CBD, CBD-loaded LNCs (F10 and F11) and CBD-functionalized CBD-loaded LNCs (F17 and F18) were assessed for cytotoxicity against human glioblastoma U373MG cells using an MTT assay. Briefly, U373MG cells were seeded into 96-well plates at a density of 2 x 10^4 cells/well. After cells had been confluent for 48 hours, they were treated with free CBD for 48 hours and with suspensions of LNCs (200 µL) for 48 and 96 hours. Then, the medium was removed and 60 µL of MTT solution (1 mg/mL) in complete DMEM were added to each well and incubated for 4 hours. Afterwards, the media containing the MTT was removed and 100 µL of DMSO was added to each well. The plates were agitated for 10 minutes and the absorbance was measured at 570 nm using a microplate reader (Varioskan Flash, Thermo Scientific). Experiments were performed in triplicate at each time-point. For each formulation of CBD-loaded LNCs, U373MG cells treated with their blank counterparts served as control. Cell viability of each group was expressed as a percentage relative

to that of control. The half-maximal inhibitory concentration (IC_{50}) was calculated in each case for comparison purposes.

2.6. *In vitro* cellular uptake

2.6.1 Uptake experiments evaluated by flow cytometry

To quantitatively evaluate the glioma targeting ability of LNCs *in vitro*, U373MG cells were seeded into 6-well plates at a density of 2.5 x 10^5 cells/well. After cells had been confluent for 48 hours, the culture medium was replaced by DiO-labeled LNCs (F13-F16 at an equivalent dye concentration of 1.65 µg DiO/mL of suspension) suspended in complete DMEM (2 mL) wherewith cells were incubated for 24 hours. Then, cells were rinsed with HBSS, trypsinized and finally resuspended in 0.3 mL of HBSS. The fluorescence intensity of cells treated with fluorescent-LNCs was analyzed with a flow cytometer (Beckman Coulter Epics XL). Experiments were performed in triplicate. U373MG cells treated with blank LNCs served as control. Cellular uptake of each group was expressed as fold-increase in mean fluorescence relative to that of control after correction for the different amount of dye per individual LNC in each formulation.

2.6.2. Uptake experiments evaluated by confocal microscopy

To qualitatively illustrate the glioma targeting ability of LNCs *in vitro*, U373MG cells were seeded into chamber slides at a density of 2 x 10^4 cells/well. After cells had been confluent for 48 hours, the culture medium was replaced by undecorated or CBD-functionalized DiO-labeled LNCs at an equivalent dye concentration of 1.65 µg DiO/mL suspended in complete DMEM (0.35 mL) wherewith cells were incubated for 24 hours. Then, cells were rinsed with HBSS and mounted with Vectashield® with DAPI mounting medium. The cells were then observed with a confocal microscope (Leica TCS SP5, 405 nm for DAPI, 488 nm for DiO). U373MG cells treated with blank LNCs served as control.

2.7. Statistical analysis

All experiments were done in triplicate and all data are expressed as mean ± SEM. Unpaired Student's t test was used for two-group analysis. Statistical significance was fixed as *:$p<0.05$, **:$p<0.01$,***:$p<0.001$. All the data were analyzed using the GraphPad Prism 7 software.

3. Results and discussion

Blank monodisperse LNCs were obtained by the PIT method in different sizes by varying the relative proportion of excipients as detailed in Table 1 (F1-F3). In formulations F4-F6, CBD was included in the formulation procedure as drug payload dissolved in the oily phase of the core of the capsules at a concentration of 15 % CBD/Labrafac® WL1349 (w/w). The choice of the oily phase was based on the solubility of CBD to easily achieve both high encapsulation efficiencies and drug loading. In this regard, whereas the authors that tried to encapsulate distinct cannabinoids in polymer nanoparticles only achieved encapsulation efficiencies around 70% [15, 16, 21], those studies that utilized lipid-based carriers exhibited values above

90% [17, 22]. This comparison has been corroborated by Durán-Lobato et al [23]. Unlike these authors, we utilized a low-energy method to prepare monodisperse lipid carriers in smaller sizes. The high incorporation efficiencies reported herein (Table 2) are in agreement with those values achieved for the incorporation of drug substances with similar log P values into analogous carriers [24, 25] and significantly higher than those obtained with less lipophilic drug substances, as etoposide with a log P= 1.1 only achieved a 56% of incorporation efficiency [26]. However, whereas these authors achieved at best a drug loading of 1.5% [25], we have utilized herein much higher percentages of CBD content (Table 2, F4-F6).

According to our size distribution measurements, for all these CBD-loaded formulations (F4-F6) there was a statistically significant increase in particle size that progressively augmented with the initial size of blank LNCs (Fig. 1a, $p<0.05$). These results are positively correlated with the respective percentage of drug loading that represented CBD in each case, which was the highest for the biggest LNCs (9.78%) and the lowest for the smallest ones (4.30%). Interestingly, the CBD loading in the oily core did not significantly alter the polydispersity index (PdI) in comparison with blank LNCs (Fig 1b, $p>0.05$). Moreover, in agreement with the hypothesized encapsulation within the oily core, no changes in the zeta potential profiles were evidenced (Fig. 1c-h). Indeed, values close to neutrality with high profile width were obtained in all cases, as it might be expected from a shell made of a complex mixture of poly (ethoxylated) surfactants (Kolliphor® HS15). Consistently, the width of the zeta potential distribution was progressively reduced with a decrease in the surfactant percentage (from the smallest (Fig. 1 c-d) to the biggest LNCs (Fig. 1 g-h)).

Moreover, to explore the potential of this phytocannabinoid to target any of the cannabinoid receptors overexpressed in glioma cells, we have developed a functionalization strategy of LNCs with CBD on their surface. This strategy consisted in the incubation of pre-formed LNCs with a CBD solution to obtain functionalized LNCs at two different concentrations of CBD (2.5 and 5 mg/mL, respectively). The incubation of LNCs with pure solvent did not contribute to any increase in particle size (data not shown). Hence, all changes observed in the characterization of LNCs were attributed to the cannabinoid itself. We followed an analogous procedure to the one utilized by other authors to incorporate novel targeting peptides on the surface of LNCs [27, 28]. However, whereas these authors only achieved 48.3% adsorption efficiency, we report herein higher incorporation efficiencies for CBD-functionalization (Table 2). These results could be explained by the lower aqueous solubility of CBD than that of peptides, which ultimately favors its adsorption to the amphiphilic surfactant interface. According to the size distribution measurements, the functionalization with CBD significantly increased the particle size of blank LNCs (Fig. 2a, $p<0.05$). This increase in average volume diameter is noticeably higher than the increase observed for CBD-loaded LNCs (F4-F6), even if the percentage of drug content is much lower in the case of CBD-functionalized LNCs (Table 2). These results supported that CBD should be placed in a distinct location than the capsule core. Indeed, the increase in volume diameter followed an inverse size-related pattern: the greatest percentage of size increase was observed with the smallest LNCs (75%) and vice versa (33% increase for medium-

sized LNCs and 16% increase for the biggest LNCs). The higher specific surface area and the higher surfactant density at the particle interface of the smallest LNCs could account for this trend observed upon CBD functionalization. Noticeably, the polydispersity index in the smallest and medium-sized LNCs was significantly increased in comparison with their blank counterparts (Fig. 2b, $p<0.01$), which did not occur when the CBD was incorporated dissolved in the oily core. Furthermore, in agreement with the hypothesized superficial location of CBD, the zeta potential profiles were remarkably smoothed in comparison to the ones previously obtained both for blank and CBD-loaded LNCs (Fig. 2 c-h). These profiles are consistent with a shell dominated by a single entity instead of the former mixture of poly (ethoxylated) surfactants and, accordingly, were steadily sharpened with an increase in CBD content in the final formulation from 2.5 mg/mL (Fig. 2 c, e, g) to 5 mg/mL (Fig. 2 d, f, h).

The different formulations of LNCs were visualized through transmission electron microscopy (TEM). Interestingly, TEM images served to evidence the spherical morphology of LNCs (Fig. 3). In no case did this geometry significantly vary upon incorporation of CBD. Moreover, the previous analysis of size distribution of the different formulations based on DLS data was highly corroborated with particle sizes observed through TEM.

Altogether, our results highlight that LNCs arise as biocompatible and biodegradable carriers for CBD, the main non-psychotropic phytocannabinoid, which will doubtless contribute to palliate the technological constraints traditionally associated with cannabinoids due to their high lipophilicity [29]. In particular, we have encapsulated CBD into the oily core of LNCs at high drug loading to attain a prolonged-release platform for this cannabinoid wherewith we will test their *in vitro* efficacy against the human glioblastoma U373MG cell line. Moreover, we have decorated the surface of LNCs with CBD wherewith subsequently conduct uptake experiments on the same human glioblastoma cell line to explore the possibilities of this cannabinoid to target *in vitro* any of the cannabinoid receptors overexpressed in glioma cells.

The fact of having obtained two distinct delivery systems with the CBD located either in the oily core or on the surface of the LNCs by varying the formulation procedure seems to refute the drop tensiometry experiments performed by some authors to elicit the disposition of a particular cargo within a core-shell carrier on the grounds of the monitored surface tension between the aqueous and oily phases upon addition of the cargo [27, 30]. These studies focus on the interactions with the aqueous and oily phases but overlook the role played by the surfactant shell in the cargo incorporation. Moreover, they underestimate the potential influence of the incorporation procedure on the final disposition of the drug substance within the carrier.

Furthermore, both untargeted and CBD-decorated fluorescently-labeled LNCs were developed for *in vitro* particle tracking purposes (F13-F16) and CBD-decorated-CBD-loaded LNCs were obtained to evidence if the CBD-decoration could enhance the *in vitro* cytoxicity of CBD-loaded LNCs. As shown in Figure 4a, after loading F1 and F2 with fluorescent dyes, we obtained analogously-sized LNCs: 20 nm (F13) and 40 nm (F14). However, the decoration of dye-loaded LNCs with CBD increased the particle size to 40 nm (F15) and 60 nm (F16), respectively. Similarly, the functionalization with

CBD of CBD-loaded LNCs (F4 and F5) significantly increased the average volume diameter to 40 nm (F17) and 60 nm (F18), respectively (Figure 4a). As observed with blank LNCs, the polydispersity index invariably increased after CBD decoration in comparison with their untargeted counterparts (Figure 4b).

In cytotoxicity experiments, the role played by particle size in the efficacy of LNCs as extended-release carriers for CBD has been evaluated with 20 nm and 50 nm-sized CBD-loaded LNCs (namely, F4 and F5).

Free CBD and the LNCs loaded with CBD within their oily core were tested for *in vitro* efficacy against the human glioblastoma U373 MG cell line by the MTT assay. Blank LNCs were used as controls for their CBD-loaded counterparts. Remarkably, blank LNCs did not show any significant cytotoxicity against the U373MG cell line within the concentration range tested (cell viability above 70% versus untreated cells according to the ISO 10993-5 Biological evaluation of medical devices, Part 5: Tests for *in vitro* cytotoxicity). Hence, all changes observed in the percentage of cell viability were attributed to the extent of CBD released from the LNCs at each time point. As other authors have previously reported that the total drug loading might play a role in the relative drug release from LNCs [31], we have normalized herein the concentration at which the drug is firstly dissolved in the oily phase (namely, 15 % of CBD/ Labrafac® WL1349 (w/w)) so that no differences in the partition gradient to the culture medium can be observed among drug-loaded formulations that could ultimately account for different release patterns. In this way, differences in the extent of CBD released will be solely dependent on the distinct release profiles from differently-sized LNCs.

Both free CBD and CBD-loaded LNCs reduced the viability of U373MG cells in a concentration-dependent manner, demonstrating thereby the *in vitro* antitumor effect of CBD against human glioblastoma. As shown in Table 3, free CBD (IC_{50} = 29.1 μM) exhibited an evident anti-proliferative effect against the U373MG cells, with an IC_{50} value in agreement with those values reported in [32]. In all cases, the inclusion of CBD within the core of the LNCs considerably increased the IC_{50} value achieved with free CBD. These results are explained by the fact that free CBD is readily available to exert its cytotoxic effect on glioma cells, whereas encapsulated CBD must be released from the oily core of LNCs firstly, a process that can be prolonged over longer periods. Other authors have recently observed analogous trends for other combinations of drug substances and carriers [33-35].

In particular, we report herein that the size of LNCs plays a pivotal role in the extent of CBD release. In this regard, based on a 48 hours treatment period, the IC_{50} of 20 nm-sized LNCs (F4) outperformed the IC_{50} value of 50-nm sized LNCs (F5): 202.6 μM vs 615.4 μM, respectively (Figure 5, Table 3). This finding highlights the distinct release patterns as a function of particle size. Moreover, we further evaluated the cytotoxic effect of these formulations over 96 hours to demonstrate if LNCs could serve as efficient prolonged-release carriers. Effectively, both formulations continued to release CBD from their oily cores and the IC_{50} values were consequently reduced with a longer treatment period (129.1 μM vs 202.6 μM for F4 and 375.4 μM vs 615.4 μM for F5). As occurred on the 48 hours treatment period, the IC_{50} values were lower for the smaller LNCs (129.1 μM vs 375.4 μM). Noticeably, regardless the incubation period, 20

nm-sized CBD-loaded LNCs (F4) achieved a 3-fold reduction in IC_{50} in comparison with 50-nm sized CBD-loaded LNCs (F5) (Table 3).

So as to determine their *in vitro* glioma targeting ability, different formulations of fluorescently-labeled LNCs at an equivalent dye concentration of 1.65 μg DiO/mL of suspension were tested on the human glioblastoma U373MG cell line by flow cytometry (Figure 6). In uptake experiments, the role played by particle size in the glioma targeting properties has been assessed separately in non-decorated and in CBD-decorated dye-loaded LNCs (namely, F13 vs F14 and F15 vs F16) and, on the other hand, the influence of CBD-decoration in glioma targeting has been evaluated for equally-sized LNCs (namely, F14 vs F15).

Overall, all tested formulations were efficiently internalized by the human malignant glioma cells, with more than 99% of positive cells in all cases. On the one hand, the influence of particle size on the extent of cellular uptake by the human glioblastoma cell line was evaluated with the purpose of determining the most auspicious features that the ideal carrier should accomplish to move forward to *in vivo* studies. This influence was evaluated both in the absence (F13 vs F14) and in the presence of the cannabinoid on the surface of the LNCs (F15 vs F16). In this regard, the measured fluorescence intensities allowed us to draw a consistent comparison of the role played by particle size for both undecorated LNCs (Figure 6a, $p<0.05$) and CBD-functionalized LNCs (Figure 6b, $p<0.001$): a decrease in volume diameter yielded an increase in *in vitro* uptake by malignant glioma cells.

On the other hand, the role played by the functionalization with CBD in the extent of *in vitro* cellular uptake was also quantitatively evaluated. The functionalization with CBD significantly enhanced the *in vitro* glioma targeting properties of LNCs, as it was concluded from a comparison of equally sized non-decorated and CBD-functionalized LNCs (F14 vs F15, Figure 6c, $p<0.001$). Altogether, the highest glioma targeting ability was achieved with the smallest cannabinoid-decorated LNC formulation (F15).

We have reported herein that the functionalization of LNCs with CBD enhanced the *in vitro* glioma targeting properties by 3.4-fold in comparison with their equally-sized undecorated counterparts. These auspicious *in vitro* glioma-targeting properties demonstrated for the CBD-functionalization strategy are in the same order of magnitude than those observed with other glioma targeting moieties [36, 37]. For instance, the aptamer AS1411 that binds to nucleolin, a protein overexpressed in highly proliferative cells yielded a 3-fold increase in *in vitro* glioma-targeting properties of poly glutamylglutamine nanoconjugates when tested in the human glioblastoma U87MG cell line [36]. With this same cell line, angiopep-2 (a targeting moiety currently in clinical trials for different brain tumor conditions that promotes receptor-mediated transcytosis through the low density lipoprotein receptor LRP1) enhanced the cellular uptake of poly (lactic-*co*-glycolic) acid nanoparticles by 3.6-fold [37]. Unlike angiopep-2, the non-peptide nature of CBD makes it less prone to cause immunogenicity.

Interestingly, CBD performed better than other tested glioma-targeting moieties. In this regard, two different ligands of the transferrin receptor, highly expressed in

glioma cells, yielded a 1.73-fold and 2.28-fold increase (for transferrin [38] and T7 peptide [39], respectively) in the cellular uptake of liposomes and core-shell nanoparticles into the C6 and U87MG cell lines. Analogously, mannose, utilized as ligand targeting the glucose transporter GLUT1, only achieved a 1.18-fold increase in cellular uptake of liposomes into the rat glioma C6 cell line [38].

Concomitantly, we have reported herein that a reduction in particle size of LNCs enhanced the cellular uptake by 3.0-fold for undecorated LNCs and 3.5-fold for CBD-decorated LNCs. In this regard, it is worth mentioning that none of the aforementioned studies evaluated the role played by particle size in the internalization extent of nanocarriers by glioma cells.

Moreover, the *in vitro* glioma targeting ability of LNCs was further analyzed qualitatively by confocal microscopy. As shown in Figure 7, both undecorated and CBD-functionalized LNCs were efficiently internalized by U373MG cells. The images taken by confocal microscopy consistently demonstrated a significantly higher glioma targeting effect for CBD-functionalized LNCs. The 3D reconstruction from the Z-stack projections corroborated that the fluorescent signal from LNCs localized in the intracellular compartment of the human glioblastoma cells, preferentially in the perinuclear region (Figure 8). A 3D video reconstruction performed by means of the LAS X software further supporting the perinuclear localization is available as supplementary material.

Given the enhancement in *in vitro* glioma targeting properties of the CBD-decorated LNCs evidenced by flow cytometry and confocal microscopy, we tested if the functionalization of CBD-loaded LNCs with CBD, with the ensuing enhanced internalization extent, could further reduce the IC_{50} values achieved for their undecorated counterparts. As shown in Figure 9, CBD-functionalized CBD-loaded LNCs outperformed the cytotoxicity of CBD-loaded LNCs following 48 hours treatment (namely, 158.6 μM vs 202.6 μM for F17 and F4; and 513.2 μM vs 615.4 μM for F18 and F5, respectively, Table 3). These results can be accounted for by the differences in the drug release rate as a function of the distinct location of the CBD in each formulation. Whereas CBD-decorated LNCs exhibit part of the cannabinoid on their surface, and hence more prone to faster release within glioma cells, undecorated CBD-loaded LNCs have the totality of the drug encapsulated within the oily core, wherein CBD has higher solubility and calls for a longer distance for diffusion.

Altogether, results from cytotoxicity and uptake experiments are highly interrelated. On the one hand, a decrease in volume diameter yields a reduction in the IC_{50} values in cytotoxicity experiments due to the faster CBD release and an increase in the *in vitro* uptake by glioblastoma cells. Hence, the cellular uptake and the drug release rate that ultimately leads to greater cytotoxicity against glioma cells can be tailored by varying the particle size of LNCs. On the other hand, the functionalization with CBD further reduced the IC_{50} values of CBD-loaded LNCs and enhanced the *in vitro* glioma targeting properties of LNCs.

These LNCs decorated and loaded with CBD offer great promise as targeted prolonged release carriers for glioma therapy. Both localized and systemic administration can be envisioned for these carriers [40]. On the one hand, localized delivery (such as convection enhanced delivery) could be used to mechanically bypass the blood-brain barrier (BBB) and directly deliver the drug carriers to the brain tissue, where they will profit from the active targeting strategy with CBD to preferentially bind to the receptors overexpressed on the brain tumor cells. On the other hand, should the herein-described glioma targeting strategy be combined with a further targeting strategy to efficiently cross the brain endothelium, glioma therapy with these LNCs could be accomplished following intravenous administration.

Importantly, the high CBD load achieved with LNCs may serve to meet the dose requirements reported in the first clinical trials that use CBD as adjuvant therapy for patients with glioblastoma. In this respect, in the NCT01812603 clinical trial glioblastoma patients received a maximum daily dose of 30 mg of CBD (in combination with a maximum daily dose of 32.4 mg of THC and dose-intense temozolomide). Importantly, this dosing regimen including cannabinoids served to nearly double both the 1-year survival rate and the median survival time [41]. Similarly, the recent NCT03529448 clinical trial has been designed so that patients are given a maximum daily dose of 40 mf of CBD (in combination with a maximum daily dose of 40 mg of THC along with temozolomide and radiotherapy within the STUPP regime). Even more recently, the NCT03607643 clinical trial has been conceived to test the potential of CBD as a single cannabinoid as adjuvant therapy for glioblastoma. Hence, devoid of safety concerns associated with psychoactive effects of THC, this study will increase the CBD doses up to 200 mg daily (a dose requirement that could still presumably be met with encapsulation into the LNC core).

Furthermore, the extended CBD release profile observed for CBD-loaded LNCs could greatly improve the dosing regimens in clinical trials, as CBD-loaded LNCs could significantly reduce the number of administrations required (which are, respectively in the aforesaid clinical trials, up to 12 times per day in NCT01812603, three-times a day in NCT03529448 or twice daily in NCT03607643).

Moreover, the glioma targeting properties of the CBD-decoration described herein are not exclusive for encapsulation of cannabinoids. Indeed, other antitumor agents traditionally included in chemotherapy protocols (such as temozolomide) can profit from the inclusion into CBD-decorated LNCs for glioma therapy.

4. Conclusions

Although cannabinoids show auspicious pharmacological properties, their therapeutic potential has not yet been widely explored due to two main issues: their strong psychoactive effects and their high lipophilicity. Hence, precisely due to their lack of psychoactive properties, CBD can take great advantage of nanomedicine-based formulation strategies for the treatment of various pathologies. In particular, CBD has been reported to not only palliate cancer-related symptoms (such as nausea, pain or anorexia) but also promote apoptotic cancer cell death through the production of reactive oxygen species, impair tumor angiogenesis and reduce cell migration.

Therefore, CBD could serve to widen the therapeutic armamentarium for the treatment of malignant brain tumors thanks to its synergistic effects with the currently available treatments and to this end, we have encapsulated CBD into the oily core of LNCs at high drug loading and evaluated their *in vitro* efficacy as prolonged-release carriers against the human glioblastoma cell line U373MG. The *in vitro* antitumor effect of CBD against human glioblastoma has been confirmed and the size of LNCs has been evidenced to play a pivotal role in the extent of CBD release: 20 nm-sized LNCs reduced by 3.0-fold the IC_{50} value of 50-nm sized LNCs.

Moreover, since the expression of different receptors to which the cannabinoids bind is increased in glioma, CBD could actively target glioma cells. Therefore, we have functionalized LNCs with CBD and evaluated their *in vitro* glioma targeting ability with the same human glioblastoma cell line. The functionalization of LNCs with CBD enhanced the *in vitro* glioma targeting properties by 3.4-fold in comparison with their equally-sized undecorated counterparts. These glioma-targeting properties equal the enhancements obtained with some other targeting moieties such as the AS1411 and angiopep-2 (the latter has already reached the clinical trials stage) and even outperform those achieved with transferrin and mannose.

Lastly, provided that the functionalization with CBD enhances the *in vitro* glioma targeting, we further evaluated if the functionalization of CBD-loaded LNCs with CBD could further reduced the IC_{50} values achieved for their undecorated counterparts. In all cases, CBD-functionalized CBD-loaded LNCs outperformed the cytotoxicity of CBD-loaded LNCs following 48 hours treatment.

Taken together, our results offer great promise for subsequent *in vivo* evaluation of LNCs loaded and decorated with CBD.

Acknowledgements

This work was supported by the Complutense Research Fund (Ref. 16/83) and by the Santander-UCM Research Group Parenteral Administration of Drugs (GR35/10). J. A.-B. would like to thank the Spanish Ministry of Education for his contract within the Professor Training Program FPU (Ref. FPU13/02325) and for funding a research stay at L'unité Micro et Nanomédecines Biomimétiques (MINT) INSERM 1066 CNRS 6021, Université d'Angers (Ref. EST14/00229). V.S. would like to thank CIBER-BBN for support. CIBER-BBN is an initiative funded by the VI National R&D&i Plan 2008–2011 financed by the Instituto de Salud Carlos III with the assistance of the European Regional Development Fund. The authors would like to thank to Carmen Doñoro, Pedro Lastres, Maite Seisdedos and Gema Elvira from the Biological Research Center (CIB, Spanish National Research Council CSIC) for the help provided with the cell culture facilities, flow cytometry analysis and confocal microscopy, respectively.

Conflict of interest

The authors declare no competing interests.

References

[1] C.M. Andre, J.F. Hausman, G. Guerriero, Cannabis sativa: The Plant of the Thousand and One Molecules, Front. Plant Sci. 7 (2016) 19. https://doi.org/10.3389/fpls.2016.00019.

[2] S. Pisanti, A.M. Malfitano, E. Ciaglia, A. Lamberti, R. Ranieri, G. Cuomo, M. Abate, G. Faggiana, M.C. Proto, D. Fiore, C. Laezza, M. Bifulco, Cannabidiol: State of the art and new challenges for therapeutic applications, Pharmacol Ther 175 (2017) 133-150. https://doi.org/10.1016/j.pharmthera.2017.02.041.

[3] G. Velasco, S. Hernandez-Tiedra, D. Davila, M. Lorente, The use of cannabinoids as anticancer agents, Prog. Neuro-Psychopharmacol. Biol. Psychiatry 64 (2016) 259-266. https://doi.org/10.1016/j.pnpbp.2015.05.010.

[4] G. Velasco, C. Sanchez, M. Guzman, Towards the use of cannabinoids as antitumour agents, Nat. Rev. Cancer 12 (2012) 436-444. https://doi.org/10.1038/nrc3247.

[5] D.H.P. de la Ossa, M. Lorente, M.E. Gil-Alegre, S. Torres, E. Garcia-Taboada, M.D. Aberturas, J. Molpeceres, G. Velasco, A.I. Torres-Suarez, Local Delivery of Cannabinoid-Loaded Microparticles Inhibits Tumor Growth in a Murine Xenograft Model of Glioblastoma Multiforme, PLoS One 8 (2013) e54795. https://doi.org/10.1371/journal.pone.0054795.

[6] X.Y. Wu, L.J. Han, X.L. Zhang, L. Li, C.Z. Jiang, Y. Qiu, R. Huang, B.Y. Xie, Z.X. Lin, J. Ren, J. Fu, Alteration of endocannabinoid system in human gliomas, J. Neurochem. 120 (2012) 842-849. https://doi.org/10.1111/j.1471-4159.2011.07625.x.

[7] M. Nabissi, M.B. Morelli, C. Amantini, S. Liberati, M. Santoni, L. Ricci-Vitiani, R. Pallini, G. Santoni, Cannabidiol stimulates Aml-1a-dependent glial differentiation and inhibits glioma stem-like cells proliferation by inducing autophagy in a TRPV2-dependent manner, Int. J. Cancer 137 (2015) 1855-1869. https://doi.org/10.1002/ijc.29573.

[8] C. Sanchez, M.L. de Ceballos, T.G. del Pulgar, D. Rueda, C. Corbacho, G. Velasco, I. Galve-Roperh, J.W. Huffman, S.R.Y. Cajal, M. Guzman, Inhibition of glioma growth in vivo by selective activation of the CB2 cannabinoid receptor, Cancer Res. 61 (2001) 5784-5789.

[9] D.N. Louis, A. Perry, G. Reifenberger, A. von Deimling, D. Figarella-Branger, W.K. Cavenee, H. Ohgaki, O.D. Wiestler, P. Kleihues, D.W. Ellison, The 2016 World Health Organization Classification of Tumors of the Central Nervous System: a summary, Acta Neuropathol. 131 (2016) 803-820. https://doi.org/10.1007/s00401-016-1545-1.

[10] J. Aparicio-Blanco, A.I. Torres-Suárez, Managing CNS Tumors: The Nanomedicine Approach, in: L.R. Morgan (Ed.), New Approaches to the Management of Primary and Secondary CNS Tumors, InTech2017, pp. 65-94. https://doi.org/10.5772/66131.

[11] C.J. Fowler, Delta(9)-Tetrahydrocannabinol and Cannabidiol as Potential Curative Agents for Cancer: A Critical Examination of the Preclinical Literature, Clin. Pharmacol. Ther. 97 (2015) 587-596. https://doi.org/10.1002/cpt.84.

[12] I. Cherniakov, D. Izgelov, D. Barasch, E. Davidson, A.J. Domb, A. Hoffman, Piperine-pro-nanolipospheres as a novel oral delivery system of cannabinoids: Pharmacokinetic evaluation in healthy volunteers in comparison to buccal spray administration, J. Control. Release 266 (2017) 1-7. https://doi.org/10.1016/j.jconrel.2017.09.011.

[13] J.R. Xie, D.J. Xiao, J.N. Zhao, N.Q. Hu, Q. Bao, L. Jiang, L.N. Yu, Mesoporous Silica Particles as a Multifunctional Delivery System for Pain Relief in

Experimental Neuropathy, Adv. Healthc. Mater. 5 (2016) 1213-1221. https://doi.org/10.1002/adhm.201500996.

[14] L. Martin-Banderas, I. Munoz-Rubio, J. Prados, J. Alvarez-Fuentes, J.M. Calderon-Montano, M. Lopez-Lazaro, J.L. Arias, M.C. Leiva, M.A. Holgado, M. Fernandez-Arevalo, In vitro and in vivo evaluation of Delta(9)-tetrahidrocannabinol/PLGA nanoparticles for cancer chemotherapy, Int. J. Pharm. 487 (2015) 205-212. https://doi.org/10.1016/j.ijpharm.2015.04.054.

[15] E. Berrocoso, R. Rey-Brea, M. Fernandez-Arevalo, J.A. Mico, L. Martin-Banderas, Single oral dose of cannabinoid derivate loaded PLGA nanocarriers relieves neuropathic pain for eleven days, Nanomed.-Nanotechnol. Biol. Med. 13 (2017) 2623-2632. https://doi.org/10.1016/j.nano.2017.07.010.

[16] L. Martin-Banderas, J. Alvarez-Fuentes, M. Duran-Lobato, J. Prados, C. Melguizo, M. Fernandez-Arevalo, M.A. Holgado, Cannabinoid derivate-loaded PLGA nanocarriers for oral administration: formulation, characterization, and cytotoxicity studies, Int. J. Nanomed. 7 (2012) 5793-5806. https://doi.org/10.2147/ijn.s34633.

[17] E. Esposito, L. Ravani, M. Drechsler, P. Mariani, C. Contado, J. Ruokolainen, P. Ratano, P. Campolongo, V. Trezza, C. Nastruzzi, R. Cortesi, Cannabinoid antagonist in nanostructured lipid carriers (NLCs): design, characterization and in vivo study, Mater. Sci. Eng. C-Mater. Biol. Appl. 48 (2015) 328-336. https://doi.org/10.1016/j.msec.2014.12.012.

[18] X.L. He, L. Yang, M. Wang, X.Z. Zhuang, R.Q. Huang, R.R. Zhu, S.L. Wang, Targeting the Endocannabinoid/CB1 Receptor System For Treating Major Depression Through Antidepressant Activities of Curcumin and Dexanabinol-Loaded Solid Lipid Nanoparticles, Cell. Physiol. Biochem. 42 (2017) 2281-2294. https://doi.org/10.1159/000480001.

[19] A. Ligresti, L. De Petrocellis, D.H.P. de la Ossa, R. Aberturas, L. Cristino, A.S. Moriello, A. Finizio, M.E. Gil, A.I. Torres, J. Molpeceres, V. Di Marzo, Exploiting Nanotechnologies and TRPV1 Channels to Investigate the Putative Anandamide Membrane Transporter, PLoS One 5 (2010) e10239. https://doi.org/10.1371/journal.pone.0010239.

[20] D.H.P. de la Ossa, A. Ligresti, M.E. Gil-Alegre, M.R. Aberturas, J. Molpeceres, V. Di Marzo, A.I.T. Suarez, Poly-epsilon-caprolactone microspheres as a drug delivery system for cannabinoid administration: Development, characterization and in vitro evaluation of their antitumoral efficacy, J. Control. Release 161 (2012) 927-932. https://doi.org/10.1016/j.jconrel.2012.05.003.

[21] L. Martin-Banderas, I. Munoz-Rubio, J. Alvarez-Fuentes, M. Duran-Lobato, J.L. Arias, M.A. Holgado, M. Fernandez-Arevalo, Engineering of Delta(9)-tetrahydrocannabinol delivery systems based on surface modified-PLGA nanoplatforms, Colloid Surf. B-Biointerfaces 123 (2014) 114-122. https://doi.org/10.1016/j.colsurfb.2014.09.002.

[22] E. Esposito, M. Drechsler, R. Cortesi, C. Nastruzzi, Encapsulation of cannabinoid drugs in nanostructured lipid carriers, Eur. J. Pharm. Biopharm. 102 (2016) 87-91. https://doi.org/10.1016/j.ejpb.2016.03.005.

[23] M. Duran-Lobato, L. Martin-Banderas, L.M.D. Goncalves, M. Fernandez-Arevalo, A.J. Almeida, Comparative study of chitosan- and PEG-coated lipid and PLGA nanoparticles as oral delivery systems for cannabinoids, J. Nanopart. Res. 17 (2015) 61. https://doi.org/10.1007/s11051-015-2875-y.

[24] G.V.U. Gamboa, S.D. Palma, A. Lifschitz, M. Ballent, C. Lanusse, C. Passirani, J.P. Benoit, D.A. Allemandi, Ivermectin-loaded lipid nanocapsules: toward the development of a new antiparasitic delivery system for veterinary applications, Parasitol. Res. 115 (2016) 1945-1953. https://doi.org/10.1007/s00436-016-4937-1.

[25] A.C. Groo, P. Saulnier, J.C. Gimel, J. Gravier, C. Ailhas, J.P. Benoit, F. Lagarce, Fate of paclitaxel lipid nanocapsules in intestinal mucus in view of their oral delivery, Int. J. Nanomed. 8 (2013) 4291-4302. https://doi.org/10.2147/ijn.s51837.

[26] B. Saliou, O. Thomas, N. Lautram, A. Clavreul, J. Hureaux, T. Urban, J.P. Benoit, F. Lagarce, Development and in vitro evaluation of a novel lipid nanocapsule formulation of etoposide, Eur. J. Pharm. Sci. 50 (2013) 172-180. https://doi.org/10.1016/j.ejps.2013.06.013.

[27] J. Balzeau, M. Pinier, R. Berges, P. Saulnier, J.P. Benoit, J. Eyer, The effect of functionalizing lipid nanocapsules with NFL-TBS.40-63 peptide on their uptake by glioblastoma cells, Biomaterials 34 (2013) 3381-3389. https://doi.org/10.1016/j.biomaterials.2013.01.068.

[28] D. Carradori, P. Saulnier, V. Preat, A. des Rieux, J. Eyer, NFL-lipid nanocapsules for brain neural stem cell targeting in vitro and in vivo, J. Control. Release 238 (2016) 253-262. https://doi.org/10.1016/j.jconrel.2016.08.006.

[29] M.A. Holgado, L. Martin-Banderas, J. Alvarez-Fuentes, M. Fernandez-Arevalo, Neuroprotective effect of cannabinoids nanoplatforms in neurodegenerative diseases, J. Drug Deliv. Sci. Technol. 42 (2017) 84-93. https://doi.org/10.1016/j.jddst.2017.04.023.

[30] G. Bastiat, C.O. Pritz, C. Roider, F. Fouchet, E. Lignieres, A. Jesacher, R. Glueckert, M. Ritsch-Marte, A. Schrott-Fischer, P. Saulnier, J.P. Benoit, A new tool to ensure the fluorescent dye labeling stability of nanocarriers: A real challenge for fluorescence imaging, J. Control. Release 170 (2013) 334-342. https://doi.org/10.1016/j.jconrel.2013.06.014.

[31] F. Lacoeuille, E. Garcion, J.P. Benoit, A. Lamprecht, Lipid nanocapsules for intracelluar drug delivery of anticancer drugs, J. Nanosci. Nanotechnol. 7 (2007) 4612-4617. https://doi.org/10.1166/jnn.2007.006.

[32] P. Massi, A. Vaccani, S. Ceruti, A. Colombo, M.P. Abbracchio, D. Parolaro, Antitumor effects of cannabidiol, a nonpsychoactive cannabinoid, on human glioma cell lines, J. Pharmacol. Exp. Ther. 308 (2004) 838-845. https://doi.org/10.1124/jpet.103.061002.

[33] C.T. Chen, Z.Q. Duan, Y. Yuan, R.X. Li, L. Pang, J.M. Liang, X.C. Xu, J.X. Wang, Peptide-22 and Cyclic RGD Functionalized Liposomes for Glioma Targeting Drug Delivery Overcoming BBB and BBTB, ACS Appl. Mater. Interfaces 9 (2017) 5864-5873. https://doi.org/10.1021/acsami.6b15831.

[34] Z. Belhadj, M. Ying, X. Cao, X.F. Hu, C.Y. Zhan, X.L. Wei, J. Gao, X.Y. Wang, Z.Q. Yan, W.Y. Lu, Design of Y-shaped targeting material for liposome-based multifunctional glioblastoma-targeted drug delivery, J. Control. Release 255 (2017) 132-141. https://doi.org/10.1016/j.jconrel.2017.04.006.

[35] X.L. Wei, J. Gao, C.Y. Zhan, C. Xie, Z.L. Chai, D. Ran, M. Ying, P. Zheng, W.Y. Lu, Liposome-based glioma targeted drug delivery enabled by stable peptide ligands, J. Control. Release 218 (2015) 13-21. https://doi.org/10.1016/j.jconrel.2015.09.059.

[36] Z.M. Luo, Z.Q. Yan, K. Jin, Q. Pang, T. Jiang, H. Lu, X.P. Liu, Z.Q. Pang, L. Yu, X.G. Jiang, Precise glioblastoma targeting by AS1411 aptamer-functionalized poly (L-gamma-glutamylglutamine)-paclitaxel nanoconjugates, J. Colloid Interface Sci. 490 (2017) 783-796. https://doi.org/10.1016/j.jcis.2016.12.004.

[37] Z.M. Luo, K. Jin, Q. Pang, S. Shen, Z.Q. Yan, T. Jiang, X.Y. Zhu, L. Yu, Z.Q. Pang, X.G. Jiang, On-Demand Drug Release from Dual-Targeting Small Nanoparticles Triggered by High-Intensity Focused Ultrasound Enhanced

Glioblastoma-Targeting Therapy, ACS Appl. Mater. Interfaces 9 (2017) 31612-31625. https://doi.org/10.1021/acsami.7b10866.

[38] X. Ying, H. Wen, W.L. Lu, J. Du, J. Guo, W. Tian, Y. Men, Y. Zhang, R.J. Li, T.Y. Yang, D.W. Shang, J.N. Lou, L.R. Zhang, Q. Zhang, Dual-targeting daunorubicin liposomes improve the therapeutic efficacy of brain glioma in animals, J. Control. Release 141 (2010) 183-192. https://doi.org/10.1016/j.jconrel.2009.09.020.

[39] L. Wei, X.Y. Guo, T. Yang, M.Z. Yu, D.W. Chen, J.C. Wang, Brain tumor-targeted therapy by systemic delivery of siRNA with Transferrin receptor-mediated core-shell nanoparticles, Int. J. Pharm. 510 (2016) 394-405. https://doi.org/10.1016/j.ijpharm.2016.06.127.

[40] J. Aparicio-Blanco, A.I. Torres-Suarez, Glioblastoma Multiforme and Lipid Nanocapsules: A Review, J. Biomed. Nanotechnol. 11 (2015) 1283-1311. https://doi.org/10.1166/jbn.2015.2084.

[41] C.A. Dumitru, I.E. Sandalcioglu, M. Karsak, Cannabinoids in Glioblastoma Therapy: New Applications for Old Drugs, Front. Molec. Neurosci. 11 (2018) 7. https://doi.org/10.3389/fnmol.2018.00159.

Excipient	F1	F2	F3	F4	F5	F6	F7	F8	F9	F10	F11	F12	F13	F14	F15	F16	F17	F18
Kolliphor® HS15	1934	846	484	1934	846	484	860	376	215	645	282	161	1934	846	645	282	645	282
Lipoid® S75	75	75	75	75	75	75	33	33	33	25	25	25	75	75	25	25	25	25
NaCl	89	89	89	89	89	89	40	40	40	30	30	30	89	89	30	30	30	30
Labrafac® lipophile WL 1349	846	1028	1209	846	1028	1209	376	457	537	282	343	403	846	1028	282	343	282	343
Water	6056	6962	7143	6056	6962	7143	2691	3094	3175	2018	2320	2381	6056	6962	2018	2320	2018	2320
CBD	-	-	-	127	154	181	10	10	10	15	15	15	-	-	15	15	57	66
DiO	-	-	-	-	-	-	-	-	-	-	-	-	12	15	4	5	-	-

Table 1: Detailed excipient weight (in mg) for each formulation of LNC in final suspension.

LNC formulation	IE (%)	DC (%)
F4	96.75 ± 1.45	4.30 ± 0.07
F5	96.43 ± 3.25	7.66 ± 0.30
F6	95.38 ± 1.25	9.78 ± 0.13
F7	94.17 ± 1.54	0.76 ± 0.02
F8	98.91 ± 2.75	1.16 ± 0.02
F9	95.22 ± 0.78	1.21 ± 0.01
F10	96.99 ± 2.58	1.55 ± 0.07
F11	95.97 ± 4.72	2.17 ± 0.06
F12	98.61 ± 2.02	2.51 ± 0.06

Table 2: Incorporation efficiencies (IE) and drug content (DC) of the different LNCs following the distinct strategies to incorporate CBD discussed in the text.

Formulation and time	**IC_{50} (μM)**
Free CBD 48h	29.1
F4 48h	202.6
F4 96h	129.1
F5 48h	615.4
F5 96h	375.4
F17 48h	158.6
F18 48h	513.2

Table 3: IC_{50} values of free CBD and the different CBD-loaded LNCs against the U373MG cell line.

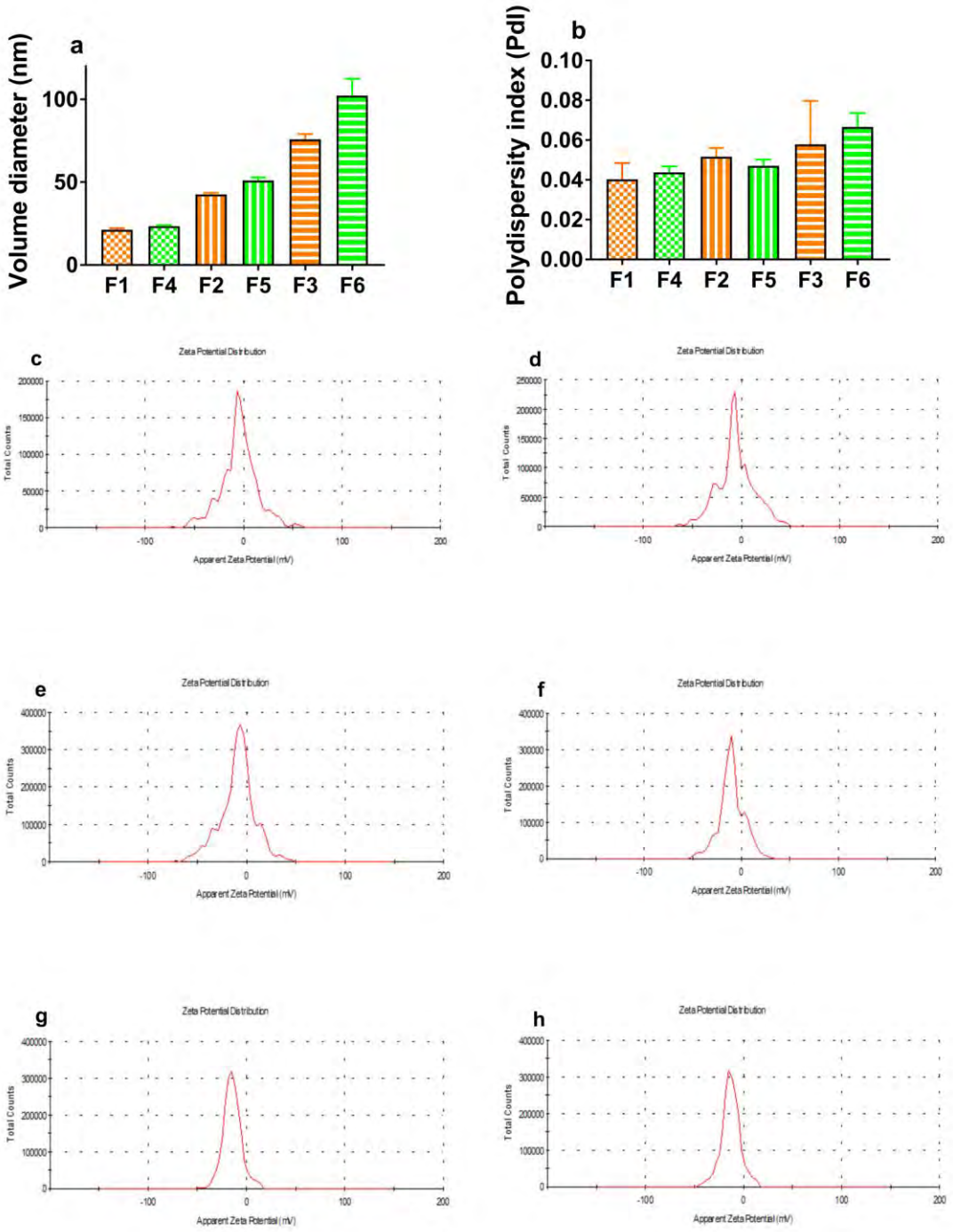
a
Volume diameter (nm)
100
50
0
F1 F4 F2 F5 F3 F6
b
Polydispersity index (PdI)
0.10
0.08
0.06
0.04
0.02
0.00
F1 F4 F2 F5 F3 F6
c
d
e
f
g
h
Zeta Potential Distribution
Total Counts
Apparent Zeta Potential (mV)

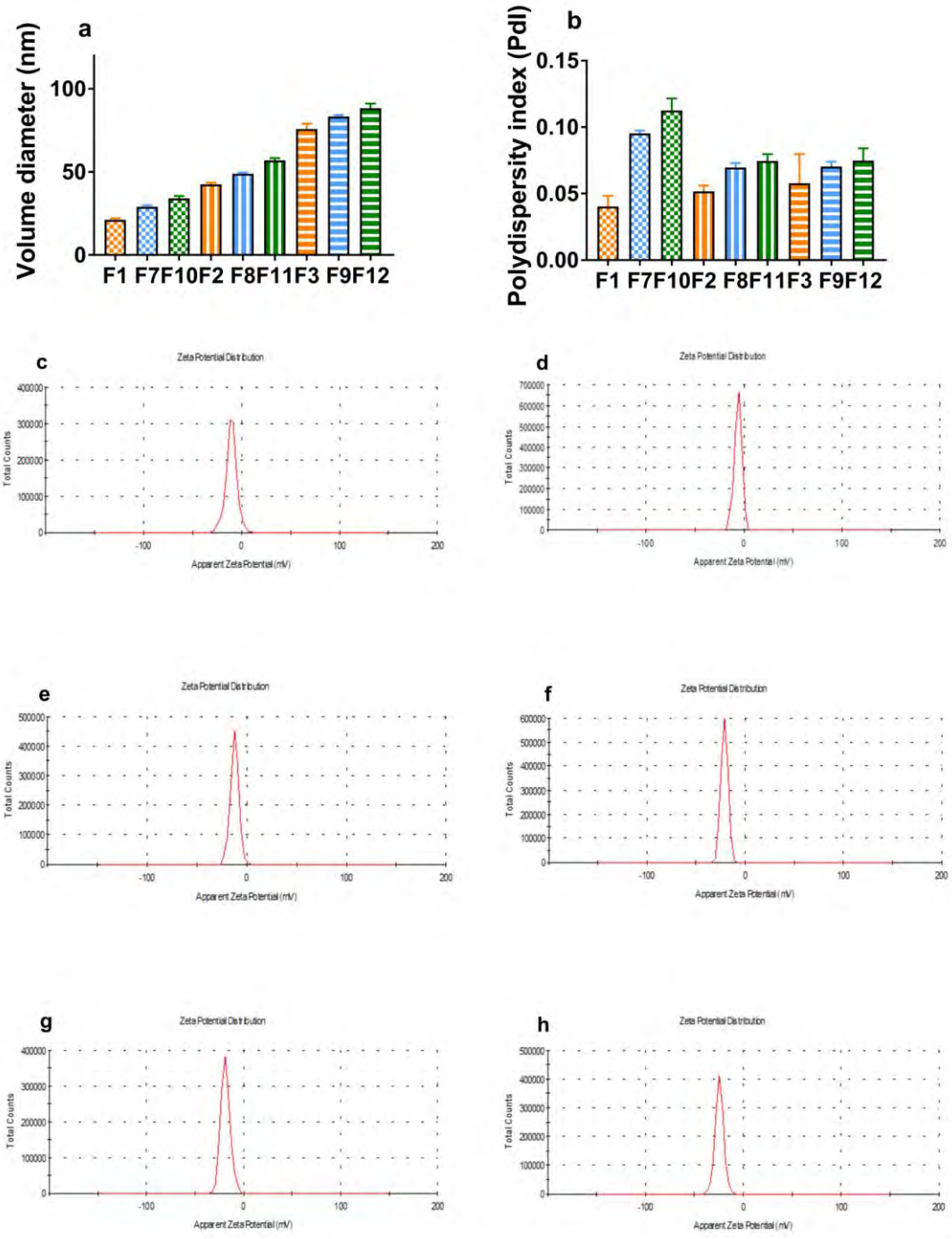
a
Volume diameter (nm)
100
50
0
F1 F7F10F2 F8F11F3 F9F12
b
Polydispersity index (PdI)
0.15
0.10
0.05
0.00
F1 F7F10F2 F8F11F3 F9F12
c
Zeta Potential Distribution
Total Counts
Apparent Zeta Potential (mV)
d
Zeta Potential Distribution
Total Counts
Apparent Zeta Potential (mV)
e
Zeta Potential Distribution
Total Counts
Apparent Zeta Potential (mV)
f
Zeta Potential Distribution
Total Counts
Apparent Zeta Potential (mV)
g
Zeta Potential Distribution
Total Counts
Apparent Zeta Potential (mV)
h
Zeta Potential Distribution
Total Counts
Apparent Zeta Potential (mV)

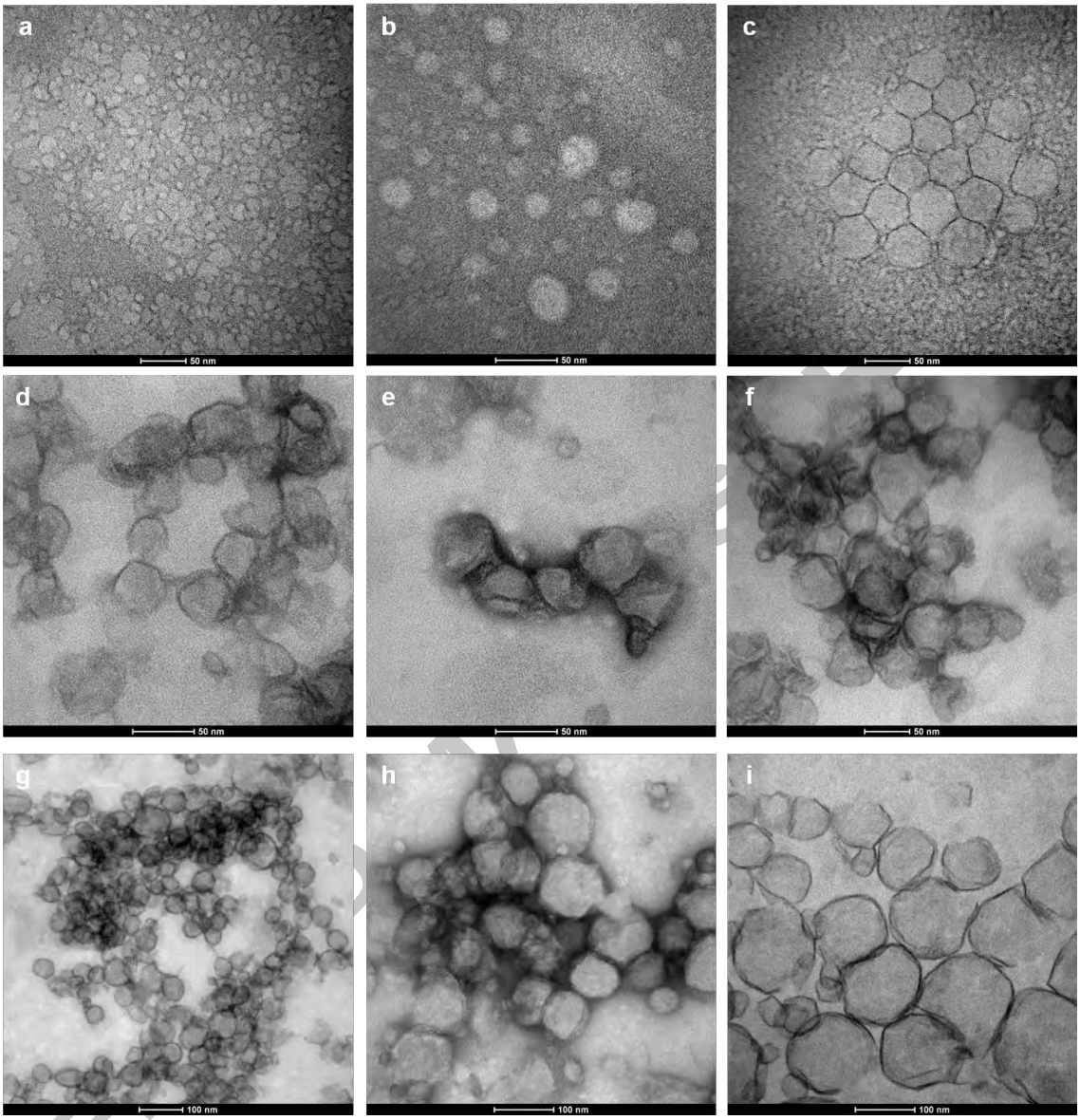

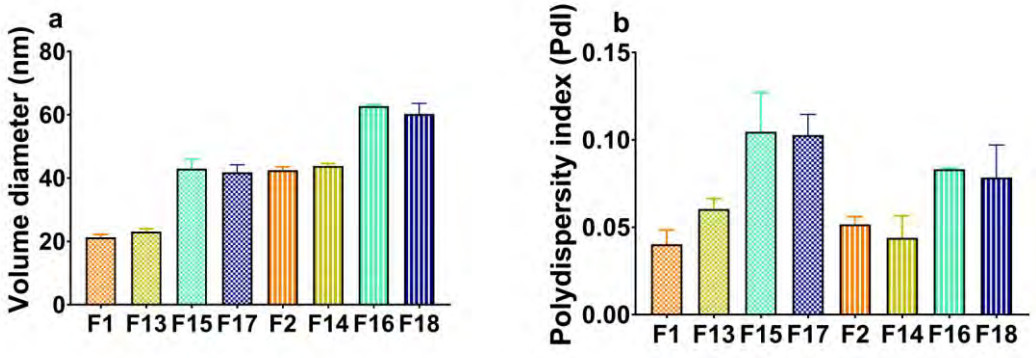

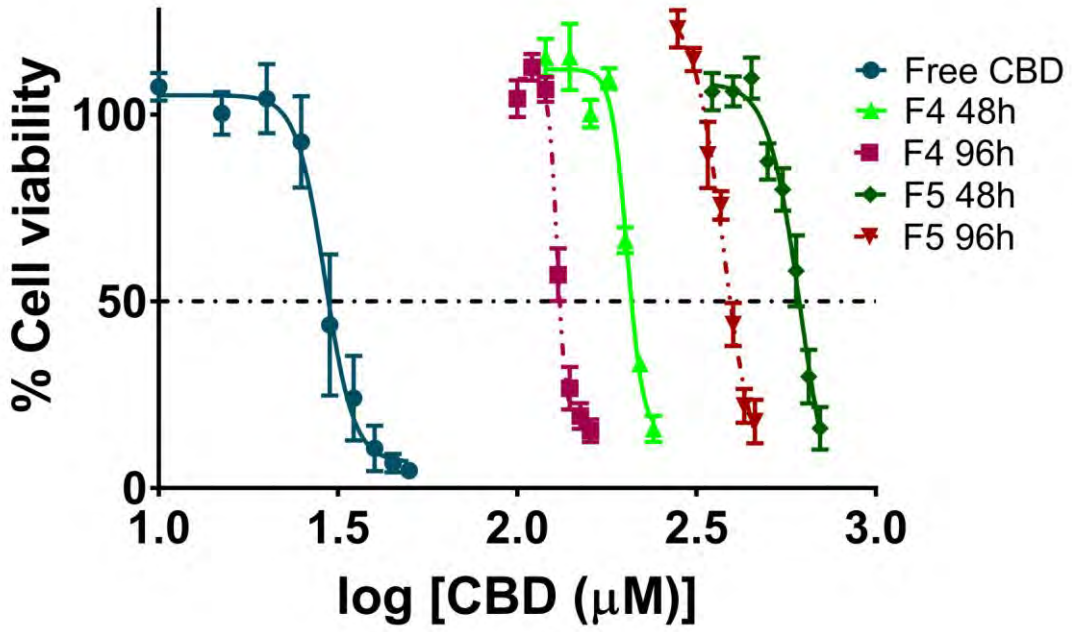

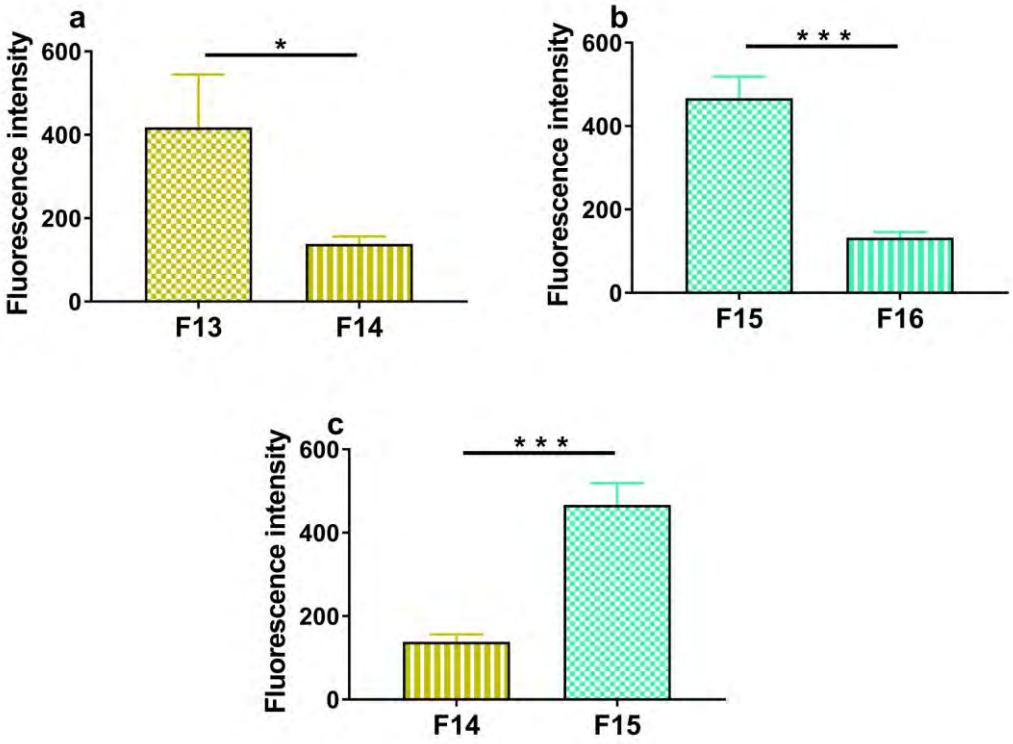

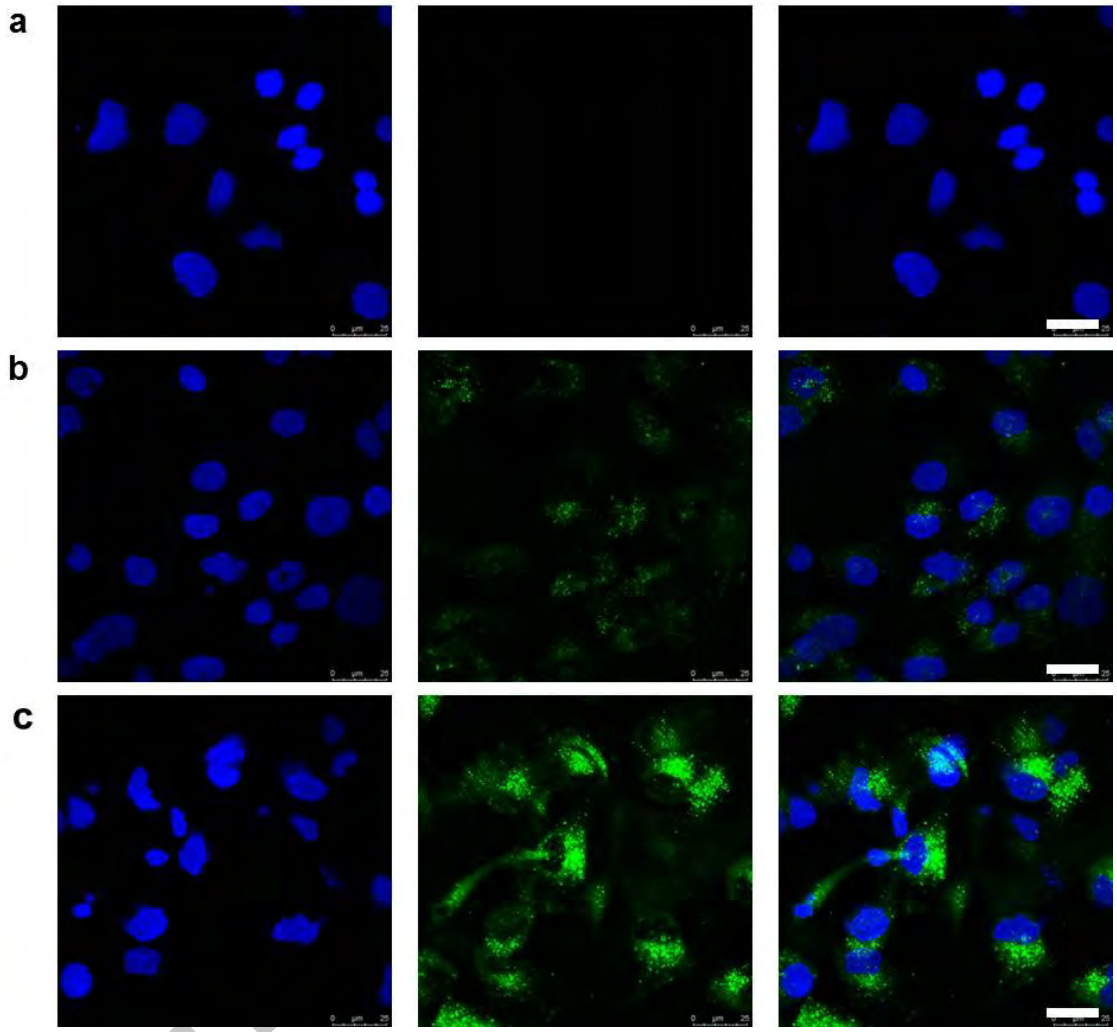

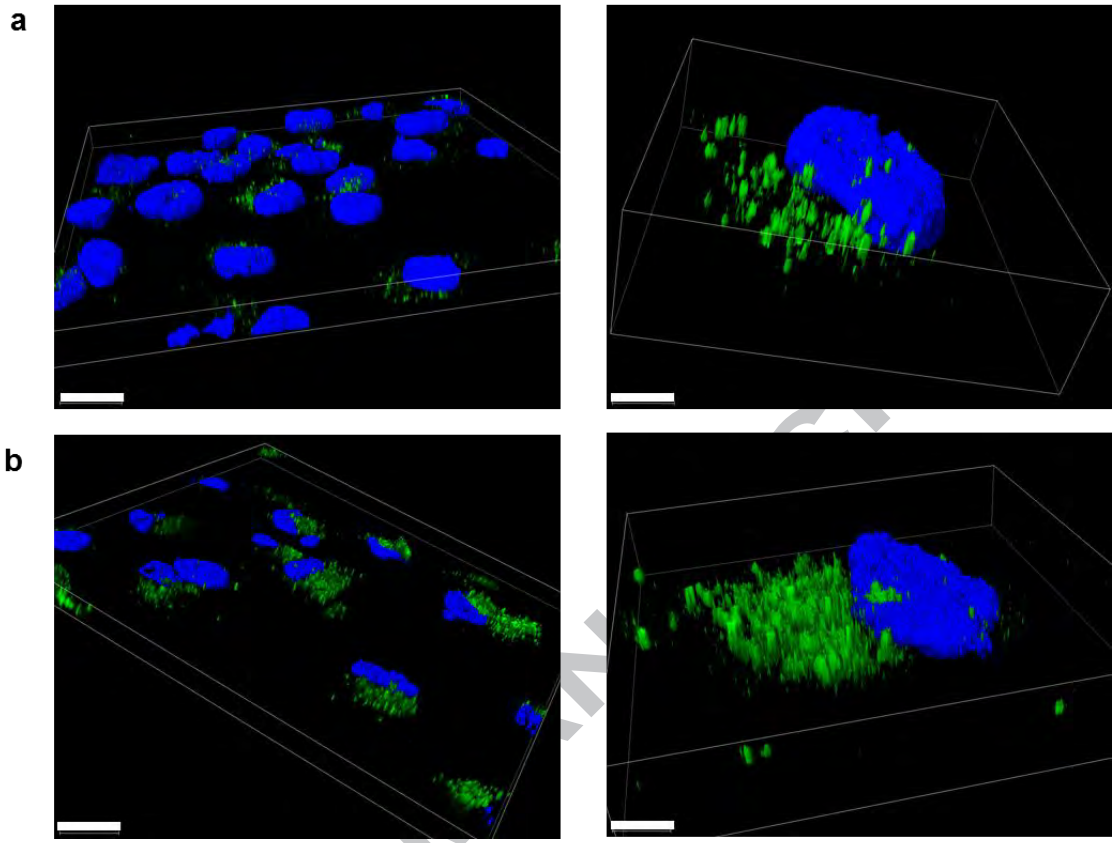

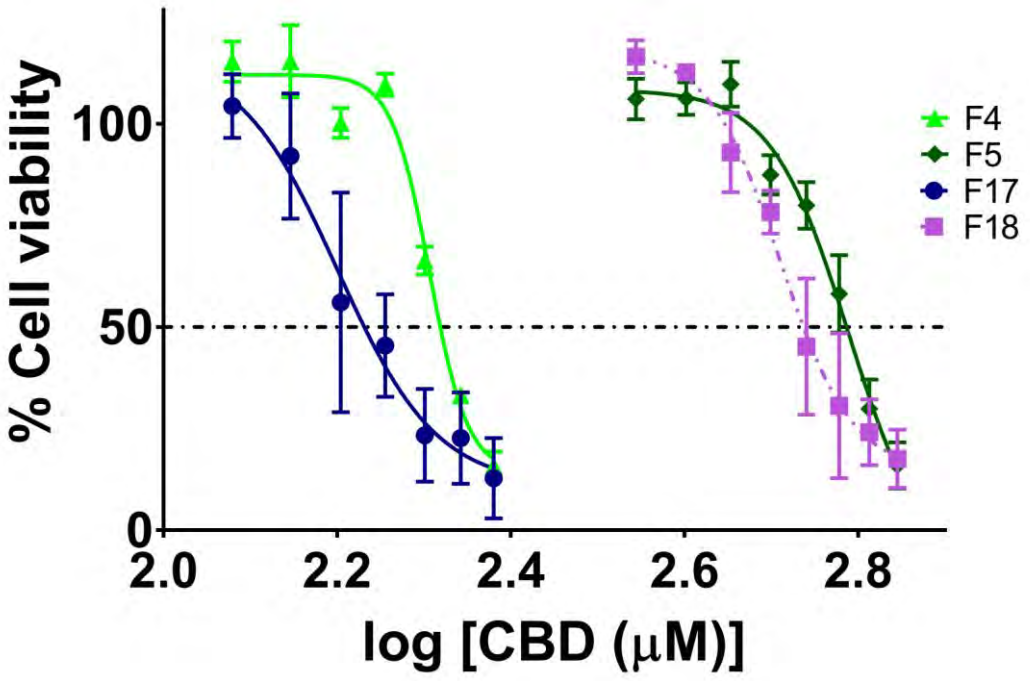

Graphical abstract